JOURNAL OF SOLID STATE CHEMISTRY 52, 313–319 (1984)

The Structure of Ce-Doped $Bi_2(MoO_4)_3$ as Determined by Neutron Profile Refinement

RAYMOND G. TELLER, JAMES F. BRAZDIL, AND ROBERT K. GRASSELLI

Sohio Research Center, 4440 Warrensville Center Road, Cleveland, Ohio 44128

AND ROBERT THOMAS, LESTER CORLISS, AND JULIUS HASTINGS

Department of Chemistry, Brookhaven National Laboratory, Upton, New York

Received May 3, 1983; in revised form July 25, 1983

The structure of $Bi_{1.8}Ce_{0.2}(MoO_4)_3$ has been refined with powder neutron diffraction data by the Rietveld method. The structure can be derived by severely distorting the scheelite structure (AMO_4) and is perhaps better written $A_{2/3}\emptyset_{1/3}MO_4$, where $\emptyset$ = cation vacancy. Of the two bismuth atom sites, cerium preferentially occupies the more symmetric of the two (Bi(2) in the structure) with some cerium found in the scheelite subcell vacancies also. This site preference is understood by examining the symmetries of the two Bi sites. Crystal data: monoclinic, space group $P2_1/c$, $Z = 4$, $a = 7.697(2)$, $b = 11.535(3)$, $c = 11.944(3)$, $\beta = 115.19$.

Introduction

The catalytic activity of $Bi_2(MoO_4)_3$ for the oxidation of hydrocarbons is well established (*1–3*). From a fundamental point of view, the utility of this material as a model of more complex commercial catalysts may be even greater, and its structure (*4*) and oxidation kinetics (*5, 6*) have been extensively studied. Introduction of Ce into the structure (maximum solubility ~10%) confers increased catalytic activity (*7*) for the ammoxidation (O_2/NH_3) of propylene to acrylonitrile. In order to understand this phenomenon fully from a structural standpoint, and because a single-crystal X-ray diffraction study was unable to unambiguously identify site compositions, a powder neutron diffraction profile analysis of $Bi_{1.8}Ce_{0.2}(MoO_4)_3$ was carried out.

Experimental

The sample of $Bi_{1.8}Ce_{0.2}(MoO_4)_3$ was prepared by the coprecipitation method. Solutions of bismuth nitrate, cerium nitrate, and ammonium heptamolybdate in the proper stoichiometric amounts were simultaneously introduced into a beaker with stirring. The volume of the resulting water slurry was gradually (~4 hr) reduced to dryness by heating at which time it was dried at 120°C for 16 hr. After drying for 3 hr each at 290 and 425°C, the material was calcined for 16 hr at 500°C.

Powder neutron diffraction data were

0022-4596/84 $3.00

collected on approximately 5 cm^3 of this sample at Brookhaven National Laboratory at the High Flux Beam Reactor, with a vanadium cell. Neutrons at a wavelength of 1.6515 Å were selected by means of the (111) reflection of a single-crystal Ge monochromator. The diffracted beam was analyzed using the (004) reflection of a pyrolytic graphite analyzer crystal (to increase resolution). Horizontal slit collimators (20′) were used before and after the monochromator and before the analyzer; a 40′ collimator was inserted between the analyzer and detector. The data were collected in steps of 0.05° (2θ), until a preset monitor count (800K) was reached (~2.3 min).

The structure was refined with a locally modified version of DBW 3.2, a Rietveld profile analysis program. Initial values of unit cell parameters were determined in a separate powder X-ray data refinement. Initial atomic positions were taken from single-crystal X-ray work on $Bi_2(MoO_4)_3^4$, both Bi positions were initially assumed to be 10% Ce, 90% Bi. In the first refinement all nonstructural parameters were allowed to vary (2θ zero, background, half width parameters, lattice parameters, an asymmetry parameter and a scale factor), then the model parameters in subsequent refinements. Scattering lengths of 0.85, 0.55, 0.66, and 0.575 were use for Bi, Ce, Mo and O, respectively. The calculated absorption coefficient is 0.018 cm^{-1}.

Initially, x, y, z and isotropic thermal parameters and the scale factor were varied (in all refinements the thermal and positional parameter shifts of different atoms in the same site were constrained to be identical), then the occupancy parameters of the Bi and Ce atoms were allowed to vary. At this stage in the refinement the Bi occupancies totaled 1.80 but that of all the Ce was consistently below 0.20. Consequently a 3% fraction of Ce was introduced into the scheelite subcell vacancy (x = 7/12, y = 1/8, z = 5/12) and the positional and isotropic thermal parameters of this atom were refined. The resulting negative value of B_{iso} was taken as an encouraging sign and in the subsequent refinements, the isotropic thermal parameter of this atom was fixed at an average of all trivalent metal atom temperature factors. In the final refinement all parameters except the occupations of the Mo and O atoms were allowed to vary. The only other refinement constraints involved fixing the total occupancy of any site to less than or equal to one. Refinement was continued until all shift/SD ratios were less than 0.20. The final values for R_{PROF}, R_{WPROF}, and R_{Bragg} are 0.077, 0.1028 (0.088 expected), and 0.016 (784 reflections). R_{PROF} values for the high (2θ = 47.5–95°) and low (0–47.5°) angle data were 0.068 and 0.086, respectively.

To check the possibility that some Bi also exists in the scheelite vacancies, a small mole fraction of Bi was also introduced. Refinement as above, yielded a negative occupation factor for this Bi atom. Throughout the aforementioned refinements, the occupations of Bi atoms in sites 1, 2, and 3 (scheelite vacancy) were 0.92 to 0.94, 0.84 to 0.88, and −0.02, respectively. The corresponding values for Ce are 0.00 to 0.02, 0.11 to 0.14, and 0.04 to 0.06, respectively. The values reported in Table II are from the last cycle of refinement.

Figure 1 displays the observed, calculated, and difference neutron diffractogram. Final parameters of the profile refinement are reported in Table I. Final model parameters are reported in Table II and bond distances and angles are presented in Table III.

Results

The structure of $Bi_{1.8}Ce_{0.2}(MoO_4)_3$ is crudely approximated by the parent compound, $Bi_2(MoO_4)_3$ and comparisons with this structure, as determined via single-crystal X-ray diffraction (*4*), are enlightening and we have maintained the same atom numbering scheme in order to facilitate the

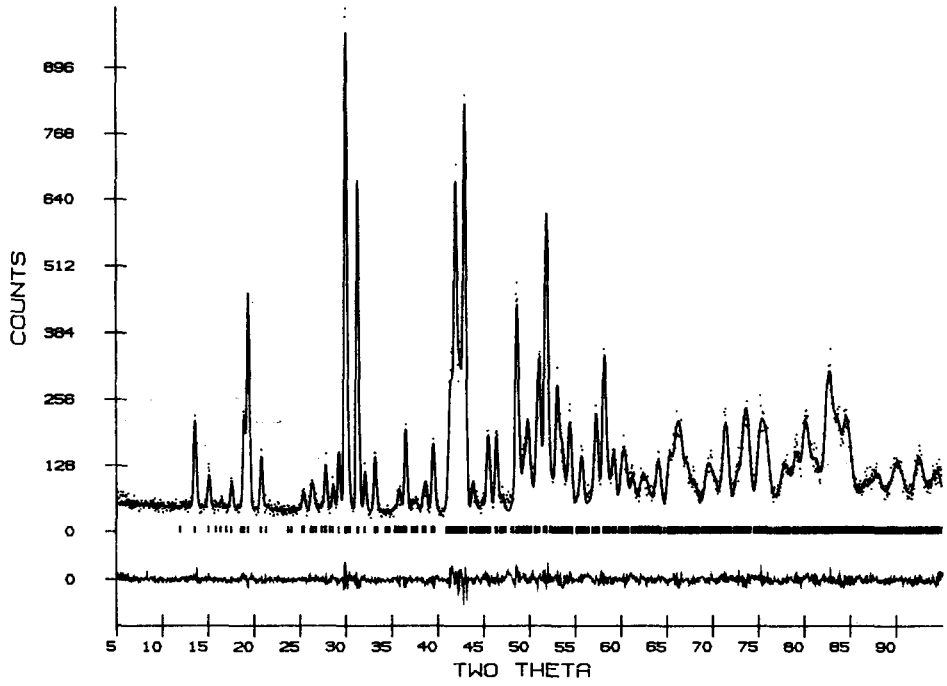

FIG. 1. Ce(10%)-doped $Bi_2(MoO_4)_3$. Profile refinement for $Bi_{1.8}Ce_{0.2}(MoO_4)_3$. The observed data are indicated by points and the calculated results by a solid line. Marks directly beneath the pattern indicate the positions of reflections. A difference curve appears at the bottom.

comparison. The structure of $Bi_2(MoO_4)_3$ is based on scheelite, ABO_4 and is perhaps better written $Bi_{2/3}Ø_{1/3}MoO_4$ where Ø represents a cation vacancy. One of the most notable distortions in $Bi_2(MoO_4)_3$ induced by the Bi occupation and vacancies is the observation of Mo dimers. Each Mo atom in $Bi_2(MoO_4)_3$ is paired with another (Mo(1)---Mo(1)' 3.41 Å, Mo(2)---Mo(3) 3.29 Å). The tetrahedral oxygen arrangement about Mo found in the ideal scheelite structure is also distorted, with a fifth oxygen atom approaching the Mo coordination sphere.

The Ce-doped system (see Fig. 2) is best represented as $(Bi_{0.94}Ce_{0.03})_a$ $(Bi_{0.88}Ce_{0.12})_b$ $(Ce_{.04})_c$ $(MoO_4)_3$ where the a, b, and c subscripts refer to the three scheelite A cation positions. Each scheelite cation position is unique, a is 94% Bi and 3% Ce, b is 88% Bi and 12% Ce, and c is mostly vacant con-

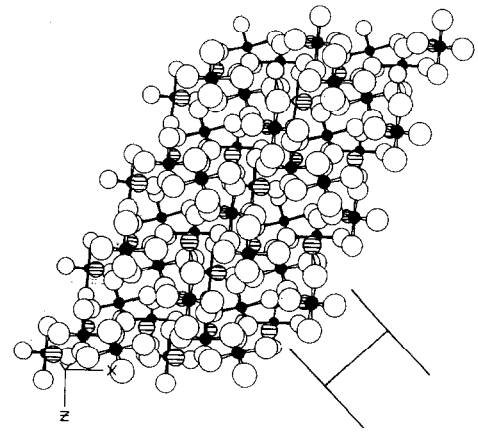

FIG. 2. Four unit cells of the [010] face of $Bi_{1.8}Ce_{0.2}(MoO_4)_3$. Molybdenum atoms are shaded, bismuth atoms are indicated with horizontal lines, and the oxygen atoms are open circles. The spacing corresponding to the scheelite subcell (~5.6 Å) is indicated.

TABLE I

DATA COLLECTION AND PROFILE REFINEMENT PARAMETERS FOR $Bi_{1.8}Ce_{0.2}(MoO_4)_3$

Space group	$P2_1/c$
Cell constants[d]	a 7.703(1)
	b 11.556(2)
	c 11.947(2)
	β 115.11(1)
Neutron wavelength	1.6515 Å
2θ Limit	95° (0.446 Å^{-1})
Background parameters[a]	A = 47.3
	B = 47.9
	C = 58.4
Half width parameters[b]	U = 1.318
	V = −.618
	W = 0.182
R_p[c]	0.077
R_{wp}[c]	0.102
R_B[c]	0.016

[a] Background = $A + Bx + Cx^2$, $x = (2\theta_i/90) - 1$.

[b] FWHM (deg) = $(U\tan^2\theta + V\tan\theta + W)^{1/2}$.

[c] The Rietveld refinement program DBW 3.2 was obtained from R. Young and D. Wiles at Georgia Technological Institute, Atlanta, Georgia and modified to fit into the local crystallographic computing system. The quantity minimized in the least squares is $\Sigma W_i(Y_i - Y_{ci})^2$ where $W_i = 1/Y_i$, Y_i = observed intensity, Y_{ci} = calculated intensity of the ith step. The profile function was assumed to be Gaussian. The reported agreement factors have the form:

$$R_p = \Sigma|Y_i - Y_{ci}|/\Sigma|Y_i|$$
$$R_{wp} = (\Sigma w(Y_i - Y_{ci})^2/\Sigma wY_i^2)^{1/2}$$
$$R_B = \Sigma|I - I_c|/\Sigma I$$

Standard deviations for parameters are calculated as

$$\sigma = a(M_{ii}^{-1}\Sigma w(Y - Y_c)^2/(N - P))^{1/2}$$

where a = code-word coefficient, M_{ii}^{-1} = diagonal element of the inverted matrix, N = number of observations, P = matrix size.

[d] Cell parameters from the powder X-ray refinement are 7.697(2), 11.535(3), 11.944(3), 115.19(2), respectively.

taining 4% Ce. The reason for this preference of Bi in the a site can be understood by examining Fig. 3. The figure displays the coordination geometry of sites a and b. The geometry of site a is that of a distorted bicapped octahedron (Bi(1), O(1), O(5), O(7), O(10) are approximately planar) with an unusually large O(1)–Bi–O(5) angle (133(1)°). The purpose of this 43° distortion from ideal square planar geometry is to accommodate the Bi lone pair (this coordination vacancy is oriented toward the viewer in Fig. 3). Site b is also eight-coordinate with a geometry of a distorted, capped pentagonal bipyramid. The atoms Bi(2), O(9), O(11), O(3), O(7), and O(6) are approximately planar. The largest angle in the pentagonal base (O(6)–Bi(2)–O(9)) is 84(1)°.

As in site a, the apparent purpose of this gap is to accommodate the Bi lone pair.

TABLE II

FINAL POSITIONAL, THERMAL, AND OCCUPANCY FACTORS FOR $Bi_{1.8}Ce_{0.2}(MoO_4)_3$

A. Positional and occupancy factors

Atom	10^3X	10^3Y	10^3Z	B150	Occ.
Bi1	262(2)	368(1)	256(1)	1.2(3)	0.94(2)
Bi2	907(2)	132(1)	77(1)	0.8(3)	0.88(2)
Ce1[a]	[a]				0.03(2)
Ce2[a]					0.12(2)
Ce3	620(34)	158(25)	492(25)	1.0	0.04(2)
Mo1	32(2)	114(1)	419(1)	0.1(3)	
Mo2	417(3)	144(2)	108(1)	4.1(5)	
Mo3	737(2)	364(1)	196(2)	2.2(5)	
O1	541(3)	58(2)	221(2)	0.9(4)	
O2	933(2)	62(2)	251(2)	0.1(5)	
O3	222(2)	198(2)	154(1)	−0.1(4)	
O4	843(2)	209(2)	407(2)	2.2(6)	
O5	221(3)	197(2)	438(2)	2.9(6)	
O6	619(3)	206(2)	64(2)	1.7(6)	
O7	950(2)	291(2)	200(2)	0.4(5)	
O8	502(2)	317(2)	204(2)	1.8(4)	
O9	288(3)	435(2)	483(1)	1.4(4)	
O10	120(2)	448(2)	77(2)	0.3(4)	
O11	844(2)	451(2)	344(2)	1.0(6)	
O12	680(2)	481(2)	98(2)	2.9(7)	

[a] The positional and thermal parameters of Ce1 and Ce2 were constrained to be identical to those of Bi1 and Bi2, respectively. The isotropic temperature factor of Ce3 was fixed at an average value of all the trivalent cations. Occupation parameters for the Mo and O atoms were fixed at 1.00.

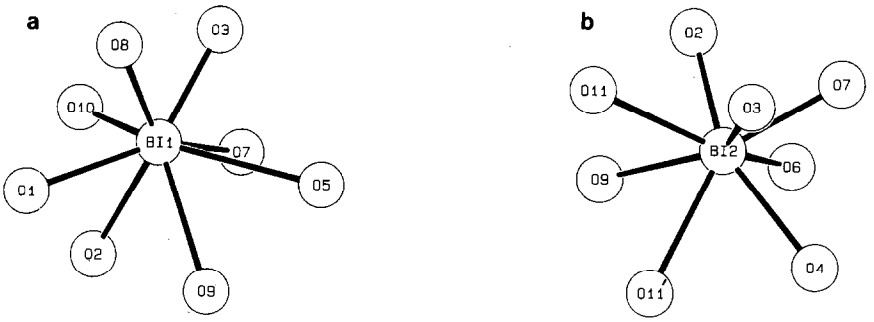

FIG. 3. (a) Site coordination about Bi(1). A large gap in the coordination sphere is oriented toward the viewer. (b) Site coordination about Bi(2).

This distortion (and the resulting "hole") is smaller than in the *a* site and is probably responsible for the preference of Bi for site *a*. Summation of the Bi–O vectors about site (1) and (2) confirm that site (1) is more asymmetric. This sum is nearly zero (~.1 Å) for site (2) and is much greater than zero for site (1) (~2.8 Å).

Distance calculations performed for site *c* indicates there is insufficient room for a trivalent Ce or Bi atom (O(6), O(12), and Mo(3) are 1.77(2), 1.98(2), and 2.24(2) Å distant, respectively). When occupied by a Ce atom the local environment about site *c* is expected to be significantly distorted from that observed in the diffraction experiment. Because site *b* is 100% occupied (by either Bi or Ce atoms) the most facile mechanism for the structure to accommodate an atom in site *c* is require site *a* to be vacant. Hence it is likely that there is a correlation between Ce occupying site *c* and Bi (or Ce) vacancy in site *a*. This represented schematically below (5a) represents the normal ordering of metal atoms on the [010] face (see Fig. 2) in the

(5a)	. . .	*M*	*M*	□	*M*	*M*	□	. . .	
(5b)	. . .	*M*	*M*	Ce	□	*M*	□	. . .	*M* = Bi/Ce
site		*a*	*b*	*c*	*a*	*b*	*c*		

compositions indicated above. Approximately 4% of the time the cation ordering is represented by (5b). The ordering in (5b) is reminiscent of that of $La_2(MoO_4)_3$ (*7*) and $Ce_2(MoO_4)_3$ (*7, 8*), a distorted scheelite structure with 1/3 cation vacancies.

The lattice parameters from the neutron refinement differ slightly from those determined from a powder X-ray refinement (see Table I). This is probably due to a small error in the neutron wavelength. The effect of Ce dopant on the $Bi_2(MoO_4)_3$ lattice parameters has been previously noted (*8*). The ionic radii of Ce^{3+} and Bi^{3+} are essentially equal but an increase in unit cell volume is observed when Ce is substituted for Bi in the structure. It had been postulated that this cell expansion was the result of a slight "dissociation" of the Mo dimers in the parent molecule. This is in fact observed in $Bi_{1.8}Ce_{0.2}(MoO_4)_3$ (Mo(2)---Mo(3) and Mo(1)---Mo(1)' are 3.38(2) and 3.43(2) Å, respectively, compared to 3.41 and 3.29 Å in $Bi_2(MoO_4)_3$. The molybdenum dimers are displayed in Fig. 4.

In the aforementioned X-ray investigation of $Bi_2(MoO_4)_3$, the results indicated that all three crystallographically distinct

TABLE III

DISTANCES (IN Å) AND ANGLES (IN DEGREES) IN $Bi_{1.8}Ce_{0.2}(MoO_4)_3$

A. Distances

Mo(1)–O(5)	1.68(3)	Bi(1)–O(10)	2.15(2)
–O(10)	1.86(2)	–O(8)	2.27(2)
–O(4)	1.78(3)	–O(3)	2.27(2)
–O(2)	1.92(2)	–O(7)	2.38(2)
–O(10)	2.27(2)	–O(1)	2.61(2)
Total bond order Mo(1) 5.6			
Mo(2)–O(1)	1.63(2)	–O(2)	2.68(2)
–O(9)	1.68(2)	–O(9)	2.74(2)
–O(3)	1.90(4)	–O(5)	3.00(2)
–O(6)	1.98(4)	Bi(2)–O(2)	2.16(2)
–O(8)	2.23(3)	–O(3)	2.32(2)
Total bond order Mo(2) 6.1			
Mo(3)–O(12)	1.72(3)	–O(7)	2.29(2)
–O(7)	1.83(3)	–O(6)	2.32(3)
–O(11)	1.87(2)	–O(4)	2.62(2)
–O(8)	1.93(3)	–O(9)	2.66(2)
–O(6)	2.34(3)	–O(11)	2.72(2)
Total bond order Mo(3) 4.9		–O(11)	2.79(2)

B. Angles about Mo atoms

Mo(1)		Mo(2)		Mo(3)	
O(5) –O(10)	99	O(1)–O(9)	108	O(12)–O(7)	110
O(5) –O(4)	107	O(1)–O(3)	103	O(12)–O(11)	96
O(5) –O(2)	105	O(1)–O(6)	101	O(12)–O(8)	106
O(5) –O(10)′	156	O(1)–O(8)	100	O(12)–O(6)	103
O(10)–O(4)	105	O(9)–O(3)	101	O(7) –O(11)	101
O(10)–O(2)	138	O(9)–O(6)	101	O(7) –O(8)	136
O(10)–O(10)′	68	O(9)–O(8)	151	O(7) –O(6)	75
O(4) –O(2)	99	O(3)–O(6)	140	O(11)–O(8)	100
O(4) –O(10)′	96	O(3)–O(8)	71	O(11)–O(6)	160
O(2) –O(10)′	77	O(6)–O(8)	74	O(8) –O(6)	72

Note. Estimated standard deviation in distances are given in parentheses. The estimated standard deviation in bond angles is 1°. Bond order (S) calculated from $S = (\text{Dist}/1.88)^{-6}$ (see Ref. (9)).

Mo atoms were chemically identical, each having two short Mo–O bonds, two of intermediate length and a fifth weakly bound oxygen ligand. This structure is represented in 6b below, as a 5-coordinate, dimolybdenyl moiety. This situation is not duplicated in the Ce-doped material however, each Mo atom is chemically distinct. While Mo(2) in $Ce_{0.2}Bi_{1.8}Mo_3O_{12}$ resembles structure 6b with two very short Mo–O bonds, the other two Mo atoms are more closely approximated by 6a. Calculations using Mo(3)–O bond lengths indicate that the total bond order about this metal is 4.9 (as compared to 5.6 and 6.1 for Mo(1) and Mo(2), respectively) (9).

Because of the inherent inability of X-ray data to allow precise oxygen location, as compared to neutron diffraction data, a high detailed comparison of the results presented here with those of the earlier reported single-crystal work on $Bi_2Mo_3O_{12}$ is problematical. If the differences are real, the calculated bond order of 4.9 for Mo(3)

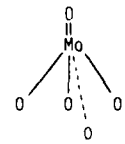

6a

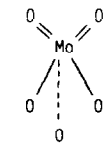

6b

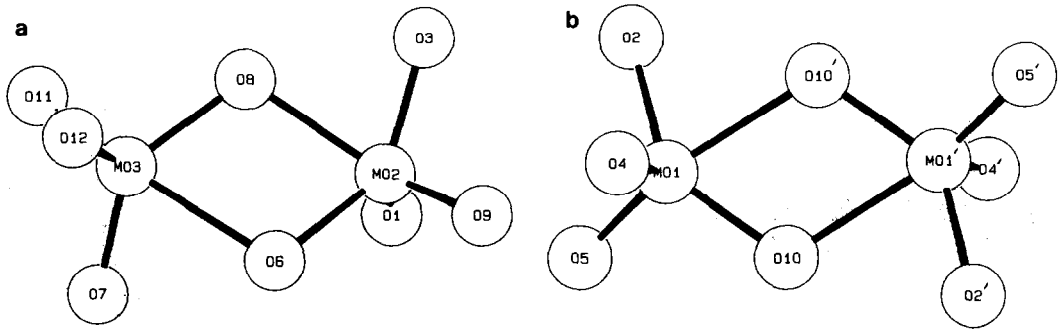

FIG. 4. Coordination geometries about the Mo atoms. (a) The Mo(2)–Mo(3) dimer. (b) A crystallographic center of symmetry exists midway between the Mo(1)–Mo(1)′ dimer.

indicates that this atom is reduced with respect to the parent compound, and that the Ce is responsible for this difference. This reduction could occur in two ways, a slight oxygen deficiency, oxidation of some Ce^{3+} to Ce^{4+}, or some combination thereof.

Summary

The effect of introducing Ce into $Bi_2(MoO_4)_3$ can be summarized as (1) a non random incorporation of Ce in scheelite cation positions with some local structural disruption when the normally vacant cation position is occupied, (2) an apparent electron transfer whereby one Mo atom is reduced with concurrent Ce^{3+} oxidation and/or oxygen removal, (3) a restructuring such that all three Mo atoms possess a unique chemical identity, and (4) the creation of two very short Mo–O bonds on Mo(2). Because two Mo–O double bonds are believed to be a necessary condition for oxidation catalysis on bismuth molybdates, this latter point may hold the key to the observed increased activity and selectivity of the Ce-doped system as compared to the parent oxide, $Bi_2Mo_3O_{12}$.

Acknowledgments

The authors are grateful to Professor E. Kostiner (Univ. of Connecticut) for helpful discussions and Ms. Linda C. Glaeser for preparing the sample of $Bi_{1.8}Ce_{0.2}(MoO_4)_3$. The research at Brookhaven National Laboratory was carried out under contract with the U.S. Department of Energy and supported by its Office of Basic Energy Sciences.

References

1. F. Veatch, *et al.* "Proceedings of 2nd Catalysis Conference, Paris (1960)."
2. G. W. Keulks, D. Krenzke, and T. M. Notormann, "Advances in Catalysis," Vol. 27, p. 183. Academic Press, New York (1978).
3. R. K. Grasselli and J. D. Burrington, "Advances in Catalysis," Vol. 30, p. 133. Academic Press, New York (1981).
4. A. F. van den Elzen and G. D. Rieck, *Acta Crystallogr. Sect. B* **29,** 2433 (1973).
5. J. F. Brazdil, D. D. Suresh, and R. K. Grasselli, *J. Catal.* **66,** 347 (1980).
6. R. K. Grasselli, J. D. Burrington, and J. F. Brazdil, *Faraday Discuss.* **72,** 203 (1981).
7. J. F. Brazdil and R. K. Grasselli, *J. Catal.* **79,** 104 (1983).
8. W. Jeitschko, *Acta. Crystallogr. Sect. B* **29,** 2074 (1973).
9. I. D. Brown and K. K. Wu, *Acta. Crystallogr. Sect. B* **32,** 1957 (1976).